Geomorphology 231 (2015) 101–115

Contents lists available at ScienceDirect

Geomorphology

journal homepage: www.elsevier.com/locate/geomorph

Laboratory simulation of debris flows over sand dunes: Insights into gully-formation (Mars)

Gwenaël Jouannic [a,b,*], Julien Gargani [a], Susan J. Conway [c], François Costard [a], Matthew R. Balme [c,d], Manish R. Patel [c,e], Marion Massé [f], Chiara Marmo [a], Vincent Jomelli [g], Gian G. Ori [h]

[a] GEOPS, Université Paris-Sud, CNRS/INSU UMR 8148, Bât. 509, 91405 Orsay, France
[b] Cerema, Direction Territoriale Est, Laboratoire de Nancy, 54510 Tomblaine, France
[c] Department of Physical Sciences, CEPSAR, Open University, Walton Hall, Milton Keynes MK7 6AA, UK
[d] Planetary Science Institute, Suite 106, 1700 East Fort Lowell Road, Tucson, AZ 85719, USA
[e] Space Science and Technology Department, STFC Rutherford Appleton Laboratory, Oxfordshire OX11 0QX, UK
[f] Laboratoire de Planétologie et Géodynamique, CNRS/INSU UMR 6112, Université de Nantes, 2 chemin de la Houssinière, BP 92205, 44322 Nantes Cedex 3, France
[g] University of Pantheon Sorbonne — Paris I, CNRS, Lab Geog, Meudon, France
[h] International Research School of Planetary Sciences, Università "G. d'Annunzio", Viale Pindaro 42, 65127 Pescara, Italy

ARTICLE INFO

Article history:
Received 10 March 2014
Received in revised form 28 November 2014
Accepted 6 December 2014
Available online 13 December 2014

Keywords:
Periglacial
Debris flow
Water
Active layer
Pore pressure
Perched channel

ABSTRACT

Gully morphology (often summarized as comprising an alcove, channel and debris apron) is one of the key elements used to support the argument for liquid water in the recent past on Mars. Nevertheless, the processes that create different gully morphologies, on both Mars and Earth, are not fully understood. One of the puzzling morphologic attributes of Martian dune gullies is their apparent lack of an apron, or terminal deposit, which has caused debate about their formation process. Several physical processes such as runoff, debris flows, granular flows, and sliding blocks falling downslope could explain the formation of these gullies. In this work, we focus on the role of liquid in the substrate as well as in the flow and choose to experimentally test the plausibility of this hypothesis. We performed a series of analogue experiments to investigate the formation of gullies on sand dune-like substrates. We used controlled flows of water over an inclined sand-box to produce gully-like forms. Ice-rich sedimentary substrates were used, including substrates that included a thin liquid water-saturated thawed layer (an 'active layer') above the ice-saturated zone to give an analogue for a 'periglacial' environment. We quantitatively demonstrate that debris flow processes in 'periglacial' experiments are conducive to the formation of narrow and long channels with small terminal deposits with perched channels. By re-analysis of Martian elevation data for dune-gullies on Mars, we have found good evidence that such terminal deposits could exist. Our experiments revealed that increased water content in the thawed layer above the frozen bed increases flow-length due to the subsequent reduction in infiltration capacity. Water is incorporated into the flow by erosion of the wet thawed layer (sand plus water) and by drainage of the thawed layer. Using a Mars environment simulation chamber, we found that atmospheric pressure conditions seem to have a limited influence on the morphology of the flows. Our experimental investigation allowed the reproduction of terrestrial debris flow and Martian gully morphologies, suggesting that a substrate that is resistant to infiltration could be present beneath the dune gullies on Mars. We suggest that, like in our laboratory experiments, the presence of ice at shallow depth is a possible explanation for the formation of these morphologies and that a wet thawed layer is a possible explanation for the long flow-length.

1. Introduction

Diverse gully morphologies occur on Mars and on Earth (Fig. 1), but the processes and climatic conditions that form the different morphologies remain poorly understood. On Mars, km-scale landforms with distinctive 'alcove-channel-debris apron' morphology are generically referred to as "gullies" (e.g., Malin and Edgett, 2000; Costard et al., 2002). Although a wide range of landforms on Mars fit this description, in general there are three main 'types' of Martian gully: (i) 'classic' gullies which have well defined alcoves, channels and aprons, and which form in bedrock or scree-like mass wasting deposits; (ii) 'pasted-on material' gullies (Fig. 1b), which have large, elongate alcoves, small channels and very small debris apron, and which form in fine-grained mantling deposits that appear to be 'pasted-on' to valley walls and impact crater inner-rims (e.g. Christensen, 2003; Aston et al., 2011); and (iii) 'dune' gullies (Fig. 1c) which have long, well defined

* Corresponding author at: Cerema, Direction Territoriale Est, Laboratoire Régional de Nancy, 54510 Tomblaine, France. Tel.: +33 383184119.
E-mail address: gwenael.jouannic@cerema.fr (G. Jouannic).

http://dx.doi.org/10.1016/j.geomorph.2014.12.007
0169-555X/

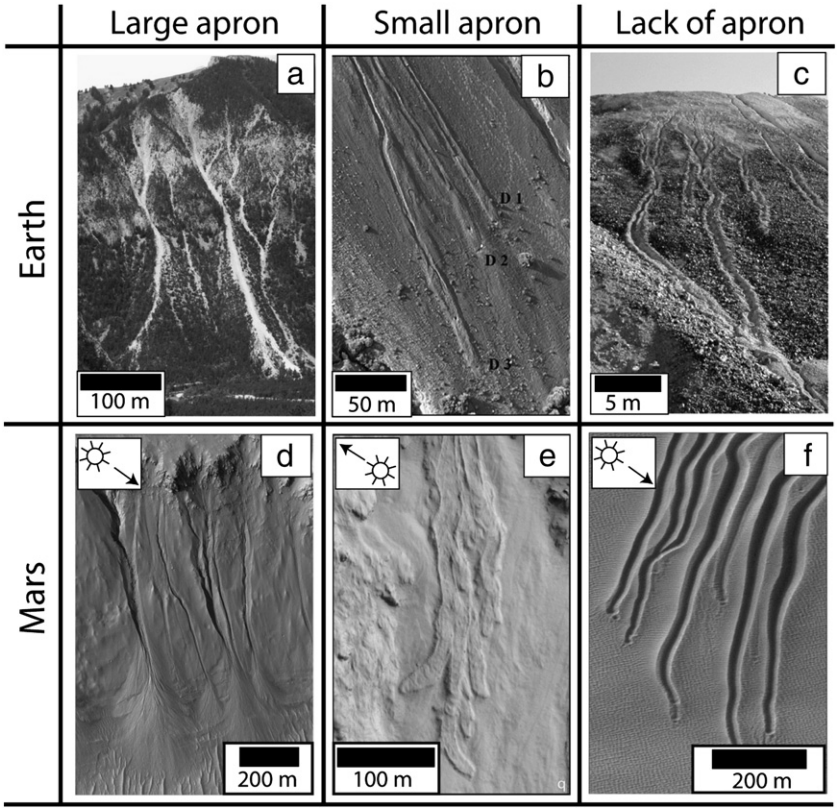

Fig. 1. Morphological comparison between terrestrial gullies and Martian analogous as a function of the apron size. (a) Debris flows in the French Alps. (b) View of debris flows at La Fossa Volcano (Vulcano island, Italy) with small aprons (from Ferrucci et al., 2005). (c) Gullies without final deposit on Earth (Photo: O. Hungr). (d) Martian gullies on slope of an impact crater (HiRISE image ESP_011727_1490). (e) Flow with digitated small aprons in the interior of Tooting crater (Morris et al, 2010). (f) Gullies without final deposit on the Russell megadune on Mars (HiRISE image PSP_007229_1255). HiRISE images credit: NASA/JPL/UofA.

channels, very small alcoves and (apparently) small to non-existent debris aprons, and which form on sand-covered slopes (most often, the slip faces of sand dunes). Here, we concentrate on Martian 'dune' gullies of the type illustrated in Fig. 1f.

The discovery of Martian gullies (Malin and Edgett, 2000) triggered numerous debates and interpretations. Several hypotheses have been suggested for the formation of gullies: (i) runoff and debris flows with liquid water from groundwater aquifers (Malin and Edgett, 2000; Heldmann and Mellon, 2004), (ii) snow-melt (Christensen, 2003; Dickson et al., 2007; Williams et al., 2009; Hauber et al, 2011), (iii) liquid CO_2 breakout (Musselwhite et al., 2001), (iv) melting of near-surface ground ice (<1 m thick) at high obliquity (Costard et al., 2002; Mangold et al., 2003; Balme et al., 2006), (v) geothermally-heated aquifers (Gaidos, 2001; Hartmann, 2001), (vi) presence of brines (Knauth et al., 2000; Knauth and Burt, 2003; Chevrier et al., 2009), (vii) processes involving CO_2 frost (Hoffman, 2002; Ishii and Sasaki, 2004; Cedillo-Flores et al., 2011), or CO_2 blocks falling down slope (Diniega et al., 2013). The availability of High Resolution Imaging Science Experiment (HiRISE) images (McEwen et al., 2007) and HiRISE Digital Terrain Models (DTM) has allowed the morphology of the gullies to be characterized in more detail than ever before (e.g., Mangold et al., 2003; Pelletier et al., 2008; Kolb et al., 2010; Lanza et al., 2010; Mangold et al., 2010; Conway et al., 2011a).

On Earth, there are many examples of gullies that are similar in morphology to 'classic' Martian gullies, especially in periglacial environments (Fig. 1; Jomelli and Francou, 2000; Costard et al., 2002; Hauber et al., 2011; Sattler et al., 2011), but only a few landforms resembling Martian dune gullies have been observed (e.g. Fig. 1c). These include gullies on dunes that are in (i) arid environments and formed by granular flow process (Cunene Sand Sea in Namibia and White Sand in New Mexico; Horgan and Bell, 2012) or (ii) cold-climate regions and formed by sand–water flows (Hugenholtz et al., 2007; Hooper and Dinwiddie, 2014).

Even if several physical processes could explain the formation of gullies, we have chosen to focus our study on the role of the liquid contained into the substrate to test the role of this mechanism and the feasibility of this process. Several studies (Costard et al., 2002; Mangold et al., 2003) have suggested that the formation of 'classic' Martian gully morphologies involves flows with a significant proportion of liquid, as indicated by the presence of sinuosity and tributary/distributary systems. However, the apparent lack of well-developed terminal deposits on dune gullies and their long runout distances (~2 km) over gentle slopes (8–10°) are hard to reconcile with any given formation process (Jouannic et al., 2012a). Dry sand experiments could trigger the formation of scars, levees and channels but only on steep slopes of 30° (McDonald and Andersen, 1996) and their morphologies are very different (Sutton et al., 2013a,b) from gullies observed on the Martian Russell megadune (Mangold et al., 2003; Jouannic et al., 2012a). For example, the gullies on Matara Crater dunes and the Russell crater megadune have features characteristic of liquid water flow (sinuosity, tributaries, distributaries), but their lack of well-developed terminal deposits is inconsistent with water flow and has led people to cite dry processes, such as sliding CO_2 blocks (e.g., Diniega et al., 2013). The presence of lateral levees on either side of these gullies has led some authors to suggest debris flow as a viable option (Mangold et al., 2003; Reiss and Jaumann, 2003; Jouannic et al, 2012a) and this could offer a solution to these apparently conflicting observations.

Debris flow (a non-Newtonian flow process comprising a sediment–water mix; Iverson, 1997) is a common process attributed to gully formation on both Earth and Mars (Coussot and Meunier, 1996; Mangold et al., 2003; Jouannic et al., 2012a) and provides a plausible candidate for the formation of Martian dune gullies, in that it can be both erosive

and depositional, forms sinuous, leveed channels, and can occur on relatively shallow slopes. Many variables can influence the morphology of debris flows (grain size, discharge, slope, soil moisture, and pre-existing topography) and their respective influences are difficult to disentangle in the field (Coleman et al., 2009). Of particular interest as an analogue for Martian dune-gullies are observations of 'perched' channels in the terminal deposits of debris flows on Earth (Larsson, 1982; Coe et al., 2002). These are erosional channels that form within deposited sediment, but are topographically above the surrounding, pre-flow surface. Hence, they are part of the depositional system of the debris flow, but in plan-view they could be easily mistaken for part of the erosional system. If perched channels are found to occur in Martian dune gullies, this could explain why previous work has reported only limited deposits for these gullies. Examples of perched channels from La Clarée valley (French Alps) is shown in Fig. 2 and for fresh debris flows located near Ísafjörður in NW Iceland (Fig. 3) in the vicinity of flows studied by Conway et al. (2010). A V-shaped incision, or a channel, is visible in the erosional upstream zone where the flow has high energy (Fig. 2a). A U-shaped channel (Fig. 2b) is present on gentler slopes in the downstream zone and in this part of the debris flow no erosion occurred, but simply deposition of lateral levees. In the terminal part of the flow, a perched channel is present (Figs. 2b, c and 3). Field observations of the foot of trees located inside the channel of the gully covered by the sediments deposited under the channel confirmed that the bottom of the channel is at higher elevation than the surrounding topography (Fig. 2c). Hence, for debris flows, the presence of a channel is not a solely sufficient indicator of erosion. A channel can still be present even though there is no net erosion, or any erosion at all.

Perched channels of this kind within debris flows tend to occur in periglacial environments on Earth (Larsson, 1982), suggesting that the presence of ground ice and/or a thawed layer (a seasonally active thawed layer above permanently frozen ground) is important for generating these morphologies. We aim to explore how this idea can be applied to dune gullies on Mars using a combination of remote sensing and laboratory simulation.

Preliminary laboratory simulations of this kind have been performed, including cold room experiments (Védie et al., 2008) which showed the qualitative effect of a melted surface layer (simulating the thawed layer) on the formation of gullies in sand dune slip faces. Nevertheless, the influence of the liquid water content of the thawed layer on the gully morphology has rarely been investigated (Jouannic et al., 2012b). As far as the authors know, only one Mars-relevant experiment has been performed to date to test the effect of atmospheric pressure on erosional capacity and runout distance of the flows (Conway et al., 2011b), but the experiments were not conducted considering an ice-rich sediment substrate.

In this study we explore the formation mechanisms of gullies observed on large sand dunes on Mars. Using analogue experiments we have investigated (i) the influence of atmospheric pressure (Martian/terrestrial pressure) on gully morphology; (ii) the role of the liquid water content of a thawed layer above a frozen substrate on gully morphology; (iii) the processes leading to perched channel morphologies; and (iv) the influence of desiccation/sublimation processes on the degradation of the gully morphology. Furthermore, using remote sensing and terrain analysis methods, we have reexamined dune gullies on Mars and find that several gullies contain 'perched channels' in the downstream section. Such features have rarely been described on Martian dune gullies before.

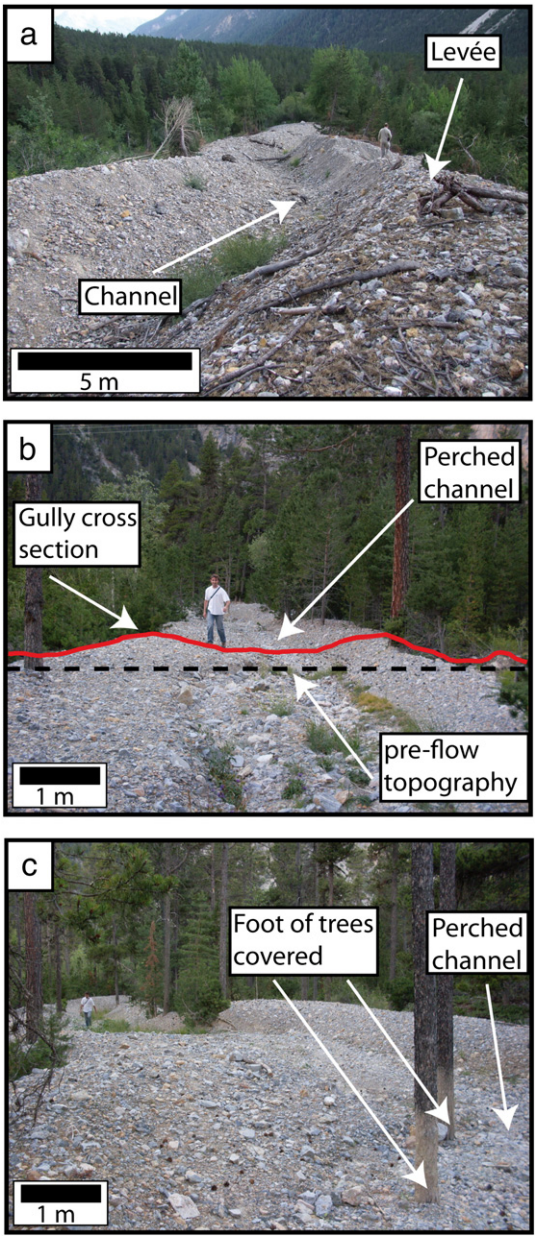

Fig. 2. Field images of debris flows in the French Alps (Clarée valley). (a) A V-shape channel profile visible in the upstream part where high energy occurred and erosion is documented. (b) A perched channel with a U-shape in the downstream part of the gully, with the cross section (red line) showing that the bottom of the channel is higher in the topography of the slope than the base surface (black dashed line). (c) The foot of the trees located inside the channel of the gully are covered by the sediments deposited under the perched channel. Photos taken by G. Jouannic and J. Gargani.

2. Methods

2.1. Martian orbital data

In order to investigate whether perched channels are present in dune gullies on Mars, we studied the Russell Crater megadune (54.5°S; 12.7°E) and a barchan dune inside Kaiser Crater (46.7°S; 20.1°E), because they both possess gullies on the dune slip faces. High Resolution Imaging Science Experiment (HiRISE) images (McEwen et al., 2007) have been used to describe gully morphology. The resolution of HiRISE images (25–100 cm pix^{-1}) permits detailed morphological observations to be made. A Transverse Mercator projection was used for all images, with the center longitude the same as the image center. We used a HiRISE digital terrain model (DTM), produced using stereo photogrammetry methods developed by the USGS (Kirk et al., 2008), to analyze the topography of the Russell Crater and Kaiser Crater dunes and their gullies. For a full description of the HiRISE DTM creation procedure, see Jouannic et al. (2012a). To study the Kaiser dune we used

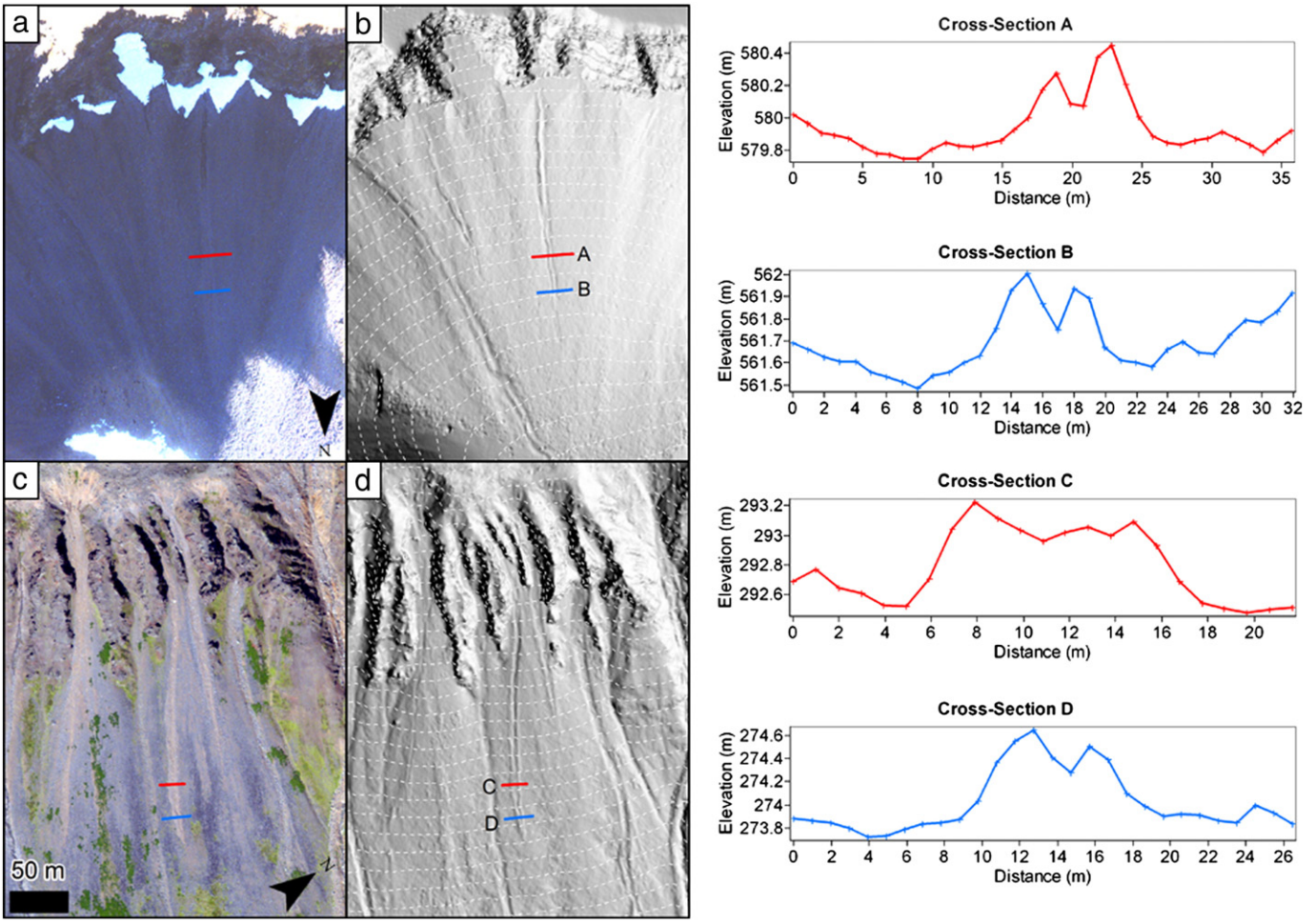

Fig. 3. Aerial images and airborne laser altimeter (LiDAR) data taken in summer 2013 for fresh debris flows located near Ísafjörður in NW Iceland in the vicinity of flows studied by Conway et al. (2010). Neither of these flows have a topographic signature in the data acquired in 2007 (Conway et al., 2010). The scale of each panel is the same as indicated in c. The images have been reoriented, so that the top of the slope is at the top of the image and hence the debris flows propagate towards the bottom of the image. The cross-sections begin at the edge with the label. The black arrows indicate the direction of the flow. (a) Orthorectified aerial image of a small debris flow on a talus slope within a cirque. (b) Shaded relief image of the LiDAR data for a, with the locations of cross sections A and B marked. White dotted lines are 10 m contours. The data from these cross sections are shown on the right. (c) Orthorectified aerial image of a small debris flow above the town of Ísafjörður, confined to the unvegetated loose talus on the upper slopes. (d) Shaded relief image of the LiDAR data for c, with the locations of cross sections C and D marked. White dotted lines are 10 m contours. The data from these cross sections are shown on the right.

a publically available HiRISE DTM (http://hirise.lpl.arizona.edu/dtm/dtm.php?ID=PSP_006899_1330).

The HiRISE DTMs are of sufficient quality and resolution to allow channels only a few meters wide to be resolved. The high resolution DTM of the Russell crater dune reveals fine-scale structures of the gullies, including lateral levees. Concerning the uncertainty of the HiRISE DTM, previous studies have estimated their vertical precision to be better than 25 cm (Pelletier et al., 2008; Mattson et al., 2011; Jouannic et al., 2012a). In this study, we considered conservative vertical uncertainties of 0.25 m in the DTMs containing the gullies of the Russell Crater megadune and the Kaiser Crater barchan.

2.2. Terrestrial orbital data

Aerial images and airborne laser altimeter (LiDAR) data were acquired on 12 August 2013 by the UK's Natural Environment Research Council's Airborne Research and Survey Facility (NERC ARSF) near Ísafjörður in NW Iceland (Fig. 3). The LiDAR instrument used was a Leica ALS50-II and the point density ranged between 1 and 4 hits m^{-2} (mean ~ 2.9). The point data were post-processed by the ARSF data analysis node (ARSF-DAN) and estimated vertical errors (taking into account between-strip errors) are ~6 cm. The data were gridded at 1 m pix^{-1} using lasTools software designed to quickly process laser altimeter data (http://www.cs.unc.edu/~isenburg/lastools). The survey included small debris flows over talus slopes located in the vicinity of flows studied by Conway et al. (2010). Neither of these flows were visible in the aerial images nor have a topographic signature in the LiDAR data acquired in 2007 (Conway et al., 2010), hence occurred between the two survey dates.

2.3. Laboratory simulations

We performed a set of debris flow experiments under Martian atmospheric pressure (~6 mbar) in the Mars Chamber (Fig. 4a) at the Open University (Milton Keynes, UK) and under terrestrial atmospheric pressure in a cold room (Fig. 4b) at the IDES laboratory (Orsay, France). One aim of this study was to characterize the influence of atmospheric pressure on gully morphology. The Mars Chamber enabled us to perform these experiments under the low pressure conditions as found at the surface of Mars, while the terrestrial cold room allowed us to perform reference experiments with an accurate control of atmospheric and frozen bed temperature, as well as control of water content inside the 'thawed layer'.

In both cases, the experiments were performed using a fine sand (200–250 μm) substrate, which had been saturated in water and completely frozen. Before some of the experiments were performed,

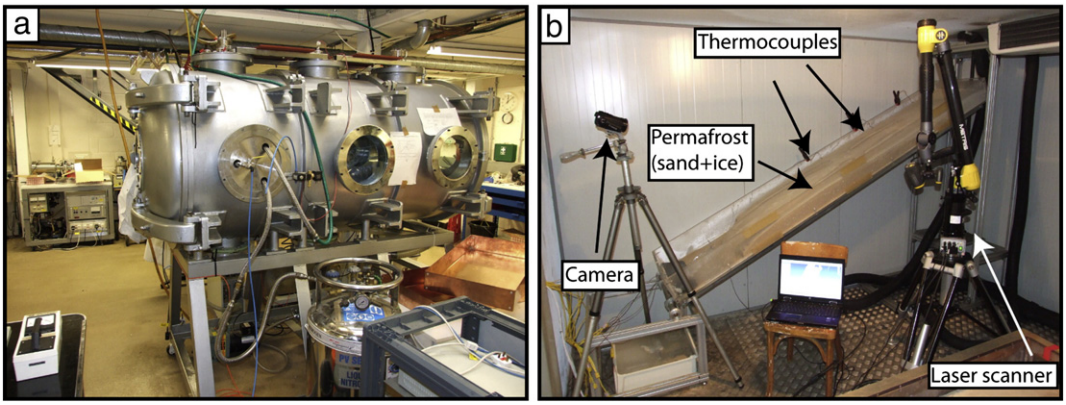

Fig. 4. Pictures of the two experimental facilities used to simulate gullies. (a) Mars Chamber in the Open University. (b) Experimental tray containing the frozen bed in the Cold room (Université Paris-Sud, France).

the uppermost few millimeters (2–6 mm) were allowed to defrost to form a thin 'thawed layer'. This creates a sandy, frozen bed with a moist surface layer, which can be inclined at various angles to produce an analogue for the slip face of a Martian or terrestrial dune.

The experiments were performed by depositing a measured amount of water at a controlled flow rate from a point source at the top of the inclined substrate. This creates a small debris flow which propagates downslope and terminates shortly after the flow of water at the top of the substrate is halted. The result of each experiment is a well-defined debris-flow landform that can include an eroded channel, levees and a blunt lobe-like debris apron. The final morphology generated by each run was precisely measured using a laser scanner. During the experimental program the following parameters were varied to explore the parameter space: discharge, slope-angle, water content of the thawed layer and thickness of the thawed layer.

The experiment allowed us to quantify the erosion and the deposition volumes, as detailed in Section 2.3.3. The water content of the thawed layer C_w was estimated measuring the ratio between weights of wet sediment $W_{\text{wet sediment}}$ and dry sediments $W_{\text{dry sediment}}$. More precisely, the water content has obtained using the equation: $C_w = (W_{\text{wet sediment}} - W_{\text{dry sediment}}) / W_{\text{dry sediment}}$.

2.3.1. Terrestrial cold room (Univ. Paris-Sud facility) experiments and procedures

To simulate a periglacial environment, a cold room large enough to accommodate an experimental slope was used (Fig. 4b). The test bed was a 2.5 m long, 0.5 m wide and 0.2 m deep rectangular tray located inside the cold room (Fig. 4b). A ~10 cm deep frozen layer composed of sand material saturated in water was placed in this tray to form the sediment substrate. Once completely frozen (after one night at −10 °C), the cold room cooling was switched off and, where appropriate for the experiment to be performed, a defrosted layer allowed to form. The surface temperature was monitored using thermocouples: the temperature of the thawed layer was ~0 °C during the experiments. Once the desired depth of melting had been achieved (after ~1–3 h), water was introduced from an external reservoir for a set duration. The temperature of the thawed layer was monitored throughout. Water was introduced from a pipe at the upper edge of the test bed and allowed to flow down and across the sediment substrate. Each experiment lasted between ~11 and ~13 s and a total of ~60 ± 10 ml of water was used for each experiment (Table 1). Two experimental runs were conducted under the same initial conditions in order to check experimental repeatability. The experiments were monitored using a video device and photographic documentation was performed for each experimental run. A peristaltic pump allowed external control over the release rate of water at ambient temperature (~15 °C). Due to the very short duration of the flow, no significant melting of the frozen bed was triggered by thermal erosion.

The depth of the melted layer was measured before and after each experiment at ~20 different points on the surface of the frozen layer. The water content of the thawed layer was calculated after each experiment by measuring the difference of the weight of a thawed layer sample with water and then without water after the complete drying of the sample using a digital balance (accuracy ~ 0.1 g). In situ laser scanning was performed before and after each experiment to generate a full elevation model of the sediment surface (vertical precision of ~0.1 mm) and to measure the elevation changes which occurred during the experiment. The propagation velocity of the flow was calculated from the video device data. The pressure in the cold chamber was at the terrestrial atmospheric pressure of 1 bar.

In order to investigate how the morphology changed as a result of desiccation, the cold room was switched on (>24 h at $T = -10$ °C) after some of the gully formation experiments. Using this protocol a dry layer of sand on top of the frozen substrate was formed. After one week, the dry layer thickness reached more than 1 cm depth.

We varied the thawed layer water content in two ways: firstly to decrease the water content we simply added a dry-sand layer to the top of the frozen layer (without letting it defrost) and secondly we added water to the thawed layer using a fine spray.

2.3.2. Description of the Mars Chamber (Open University facility)

For the Martian environment simulation experiments, the sediment bed was contained within a cylindrical low pressure chamber 2 m in length and ~1 m in diameter. The test bed is a 1 m long, 0.1 m deep rectangular metal tray. A ~5 cm deep sand bed was saturated with water, leveled off and then placed in the freezer onsite. After complete freezing of the material (after ~15 h), the tray was removed and, where necessary, a defrosted layer was allowed to form. The tray was placed in the chamber and the pressure reduced to 6 mbar (~1 h). The temperature of the frozen bed, melted layer and the chamber pressure were monitored throughout.

Once the correct pressure was achieved, water was introduced from an external reservoir. The pressure in the chamber was actively controlled using a vacuum pump and was maintained at 6 mbar for the low pressure experiments. The temperature of the surface was monitored during the experiments using thermocouples. Water was introduced from a pipe at the upper edge of the test bed and allowed to flow down and across the sediment substrate. Thus each experiment lasted between ~5 s and ~15 s and a total of ~60 ± 10 ml of water was used each time (Table 2). A solenoid valve within the end of the hose allowed external control over the release of water. The slope was controlled and three slopes were tested (15°, 20° and 25°). The progress of each experiment was monitored using two internal cameras and two external video devices. Photo-documentation was performed prior, during and after each experimental run. Once the experiment was complete the chamber was returned to atmospheric pressure (~1 min) and

Table 1
Summary of experiments performed inside the cold room (Univ. Paris-Sud facility).

Experiment name	Experiment date	Slope (°)	Water used (ml)	Flow rate (ml s^{-1})	Flow velocity (cm s^{-1})	Thawed layer thickness (mm)	Water content in the thawed layer (%)	Total flow length (cm)	Apron width (cm)	Levee thickness/levee width	Final deposit length (cm)	Flow duration (s)	Deposition (mm^3)	Erosion (mm^3)
12_06_08_1g	08/06/2012	20	109	4.3	4.6	3	/	134	/	/	/	29	/	/
12_06_08_1d	08/06/2012	20	92	4.3	5.6	3	/	129	/	/	/	23	/	/
12_06_12_1	12/06/2012	25	61	4.6	5.1	4	15	78	/	/	22.0	15	55,062	−45,726
12_06_12_2	12/06/2012	25	59	4.6	4.3	4	15	62	/	/	18.7	14	/	/
12_06_13_1g	13/06/2012	25	64	4.6	5.3	4	23	94	/	/	23.0	18	109,526	−92,140
12_06_13_1d	13/06/2012	25	60	4.6	6.8	4	23	110	/	/	22.7	16	/	/
12_06_13_2g	13/06/2012	25	59	4.6	2.6	6	0	36	/	/	14.8	14	34,069	−27,855
12_06_13_2d	13/06/2012	25	61	4.6	2.4	6	0	33	/	/	10.6	14	29,117	−23,313
12_06_14_1g	14/06/2012	25	68	4.6	5.7	4	19	90	/	/	22.8	16	82,199	−65,411
12_06_14_1d	14/06/2012	25	71	4.6	4.9	4	19	100	/	/	21.3	20	98,645	−79,150
12_06_14_2	14/06/2012	25	57	4.6	8.5	0	/	129	/	/	/	15	54,594	−39,151
12_06_15_1g	15/06/2012	25	60	4.6	4.6	5	19	68	/	/	/	15	/	/
12_06_15_1d	15/06/2012	25	58	4.6	5.7	4	19	108	/	/	/	19	109,890	−98,336
12_06_18_1g	18/06/2012	25	55	4.6	6.9	2	3	103	/	/	/	15	39,292	−29,451
12_06_18_1d	18/06/2012	25	63	4.6	3.2	2	3	44	/	/	/	14	43,140	−32,410
12_06_25_1g	25/06/2012	25	56	4.6	5.9	2	7	89	/	/	/	15	/	/
12_06_25_1d	25/06/2012	25	47	4.6	7.5	2	7	99	/	/	/	13	/	/
12_06_25_2g	25/06/2012	25	58	4.6	2.6	4	7	34	/	/	/	13	/	/
12_06_25_2d	25/06/2012	25	58	4.6	3.4	4	7	45	/	/	/	13	/	/
12_06_29_1g	29/06/2012	25	61	4.6	4.1	2	0	58	/	/	11.2	14	37,536	−34,989
12_06_29_1d	29/06/2012	25	60	4.6	4.2	2	9	59	/	/	12.5	14	44,058	−38,946
12_06_29_2g	29/06/2012	25	49	4.6	3.9	4	9	45	/	/	14.7	12	33,725	−28,629
12_06_29_2d	29/06/2012	25	56	4.6	2.8	4	9	37	/	/	11.5	13	28,754	−24,490
12_07_03_1g	03/07/2012	25	56	4.6	5.4	4	20	77	/	/	11.5	14	46,699	−45,361
12_07_03_1d	03/07/2012	25	55	4.6	7.3	4	20	108	/	/	11.2	15	64,996	−63,757
12_07_04_1g	04/07/2012	25	63	4.6	2.9	4	11	40	/	/	10.7	14	39,665	−31,060
12_07_04_1d	04/07/2012	25	63	4.6	3.3	4	11	45	/	/	9.2	14	34,955	−32,010
12_07_04_2g	04/07/2012	25	56	4.6	3.6	4	11	48	/	/	10.6	13	37,416	−33,009
12_07_04_2d	04/07/2012	25	56	4.6	3.3	4	11	43	/	/	14.1	13	31,345	−29,324
12_07_09_1g	09/07/2012	25	61	4.6	3.4	3	4	46	/	/	13.7	14	36,108	−27,047
12_07_09_1d	09/07/2012	25	62	4.6	3.2	3	4	45	/	/	14.8	14	36,680	−29,063
12_07_09_2d	09/07/2012	25	29	4.6	7.9	2	4	64	/	/	7.8	8	22,451	−17,472
11_05_18_1	18/05/2011	20	60	1.0	1.5	3	Wet	93	6.0	0.3	/	62	/	/
11_05_18_2	18/05/2011	20	120	0.9	1.0	5	Wet	136	9.5	0.2	/	131	/	/
11_05_18_3	18/05/2011	20	120	0.9	1.2	5	Wet	153	9.1	0.2	/	132	/	/
11_05_19_1	19/05/2011	20	60	0.9	1.0	5	Wet	66	6.4	0.2	/	64	/	/
11_05_19_2	19/05/2011	26	60	1.0	0.8	5	Wet	49	4.5	0.2	/	61	/	/
11_05_20_1	20/05/2011	26	94	1.5	2.2	1	Wet	141	5.1	0.5	/	63	/	/
11_05_20_2	20/05/2011	26	98	1.5	2.5	4	Wet	162	6.9	0.3	/	64	/	/
11_05_23_2	23/05/2011	20	120	1.8	2.4	3	Wet	163	7.5	0.2	/	68	/	/
11_05_26_1	26/05/2011	20	120	1.8	2.3	3	Wet	150	7.0	0.2	/	65	/	/
11_05_26_2	26/05/2011	15	120	2.1	1.9	5	Wet	107	7.6	0.1	/	56	/	/
11_05_27_1	27/05/2011	26	120	1.9	1.7	5	Wet	108	7.2	0.2	/	62	/	/
11_05_30_2	30/05/2011	26	120	1.9	2.4	3	Wet	147	4.4	0.5	/	62	/	/
11_06_09_1	09/06/2011	26	58	2.0	4.4	4	Wet	128	4.6	0.3	/	29	/	/
11_06_15_1	15/06/2011	15	240	4.2	3.0	5	Wet	172	/	0.1	/	57	/	/

the depth of the melted layer was measured. The tray was removed for scanning to generate a full elevation model of the sediment surface and to make any other additional measurements. The water content of the thawed layer was kept constant in these experiments.

2.3.3. Derivation of measured morphologic parameters

In order to obtain quantitative measurements of the experimental flow morphologies (Fig. 5a) we scanned the surface of the sand-bed after each experiment to build a digital elevation model (DEM) of the gully (Fig. 5b). We applied a natural neighbor interpolation method to the point cloud with a cell size of 0.5 mm to produce the DEMs. The DEMs were used to calculate the total volume of eroded and deposited sand. Before the experiment, the sand substrate was prepared to obtain a flat topography with a constant slope. The volume of sand eroded, or deposited, was calculated by taking the difference between an estimated initial topography and the measured topography generated by the flow (Fig. 5d). The initial topography was estimated by natural neighbor interpolation of the topographic points with the flow area masked out. The error introduced into the volume calculation by using an estimated initial surface was ~0.5%. We calculated this error by comparing volumes derived using this technique and those based on pre-scanning the initial surface for the same flow. Because the difference in the volumes calculated using the interpolation technique and pre-scanning technique were so small, pre-scanning of the bed before each experimental run was not necessary.

For the experiments under Martian conditions performed at the Open University, the bed was scanned using the David Laserscanner system (http://www.david-3d.com/). This scanning system uses a 'structured light' (Winkelbach et al., 2006) approach to generate an elevation point cloud. A fixed video camera records the progress of a laser-line over a subject — the deviation of the laser from a straight line allows estimation of the topography. To correct for camera distortion and to provide scale, an image is first taken of known-scale calibration boards with a printed black-and-white pattern. The subject is then placed between the camera and calibration boards and scanning undertaken. Linear artifacts can be introduced by high ambient light conditions and vibrations of the laser — these typically have an amplitude of ~1 mm. Because of the random distribution of these errors, this resulted in <0.5% error on the volumes calculated. Voids are caused by steep areas of topography from which no light was received and for

Table 2
Summary of experiments performed inside the Mars Chamber (Open University facility).

Experiment name	Experiment date	Slope (°)	Water used (ml)	Flow rate (ml s^{-1})	Flow velocity (cm s^{-1})	Active layer thickness (mm)	Active layer composition	Total flow length (cm)	Apron width (cm)	Levee thickness/levee width	Flow duration (s)	Deposition (mm^3)	Erosion (mm^3)
11_11_17_1	17/11/2011	20	70	8.0	4.3	4.0	Wet	47	4.3	0.3	10.9	23,632	−26,162
11_11_18_2	18/11/2011	20	65	4.3	2.6	4.0	Wet	55	4.7	0.2	21.2	24,004	−27,996
11_11_21_2	21/11/2011	20	60	6.8	4.1	4.0	Wet	63	5.3	0.2	15.5	19,950	−27,018
11_11_22_1	22/11/2011	20	50	3.5	2.3	4.0	Wet	36	5.6	0.2	15.8	19,044	−20,686
11_11_23_2	23/11/2011	20	65	11.9	6.1	4.0	Wet	55	4.7	0.3	9.0	20,307	−19,319
11_11_25_1	25/11/2011	26	55	13.3	7.1	3.0	Wet	43	4.1	0.3	6.0	13,763	−11,699
11_11_25_2	25/11/2011	26	52	10.5	6.2	3.0	Wet	46	3.8	0.3	7.5	17,346	−11,578
11_11_28_2	28/11/2011	26	55	8.6	6.3	4.0	Wet	49	3.4	0.3	7.8	20,016	−13,755
11_11_29_1	29/11/2011	26	40	6.6	4.4	2.0	Wet	30	3.7	0.2	6.9	18,285	−11,423
11_11_29_2	29/11/2011	26	60	6.0	3.1	4.0	Wet	38	4.6	0.3	12.4	29,543	−19,043
11_11_30_1	30/11/2011	26	60	5.6	3.7	2.5	Wet	52	3.0	0.3	14.2	14,848	−13,287
11_11_30_2	30/11/2011	26	60	5.6	3.1	3.5	Wet	38	5.0	0.3	12.2	21,452	−15,323
11_12_01_1	01/12/2011	26	50	4.4	1.2	6.0	Wet	15	4.0	0.6	12.3	17,226	−6802
11_12_01_2	01/12/2011	26	55	4.9	2.3	3.0	Dry	30	4.9	0.2	13.2	20,559	−16,028
12_02_24_1	24/02/2012	15	60	5.3	3.2	3.0	Wet	49	6.3	0.1	15.3	14,390	−19,699
12_02_27_1	27/02/2012	15	50	5.4	3.6	4.0	Wet	58	8.2	0.1	16.3	9974	−18,312
12_02_27_2	27/02/2012	15	55	7.5	3.7	4.0	Wet	35	4.6	0.1	9.5	16,064	−11,353
12_02_28_1	28/02/2012	20	40	7.3	4.3	4.0	Dry	30	5.2	0.2	6.9	22,965	−12,098
12_02_28_2	28/02/2012	20	70	7.3	4.1	3.0	Dry	45	5.6	0.2	11.0	31,921	−26,775
12_03_01_1	01/03/2012	15	55	11.2	6.1	4.0	Wet	41	4.6	0.1	6.7	18,858	−10,781
12_03_01_2	01/03/2012	15	65	8.7	4.1	4.0	Wet	50	5.6	0.1	12.2	18,298	−19,187
12_03_05_1	05/03/2012	20	70	13.6	9.7	3.0	Wet	50	/	/	5.1	17,045	−13,373
12_03_06_1	06/03/2012	15	150	6.3	2.1	4.0	Dry	58	4.9	0.2	27.0	76,292	−45,135
12_03_07_1	07/03/2012	20	100	7.5	3.0	4.0	Dry	46	6.4	0.3	15.1	57,757	−39,865
12_03_08_1	08/03/2012	20	45	6.7	5.1	4.0	Dry	30	2.9	0.2	5.8	20,903	−12,366

any topography near the edge of the tray — "shadows". We used a conservative estimate of ~10% for the error on the volume for the Martian chamber experiments to take into account these unquantified artifacts.

For the experiments under terrestrial conditions performed at Orsay, an industrial grade laser scanner was used (MCA Metris). This laser scanner allows a very precise measurement of the volume with a vertical uncertainty on the raw data of ~0.1 mm and a typical horizontal spacing of <0.2 mm between point samples. Due to the high point density and high vertical accuracy the error introduced by the scanner itself is below that introduced by the volume-calculation method.

Using a ruler or Vernier calipers we measured the height of the levees, the width of the levees, the width of the apron, the length of the apron the depth of the channel and the length of the flow. The apron length was measured from the beginning of the perched channel system to the end of the deposit. We estimated an error on these measurements of ~0.5 mm. We did not take these measurements from the DEM, because we could more reliably identify the edges of levees, channels and aprons necessary to perform the measurements using in-situ techniques.

3. Results

3.1. Remote sensing observations of Mars: evidence for perched channels

By analyzing HiRISE DEMs, we have found potential perched channels in several dune gullies on Mars. On the Russell megadune we

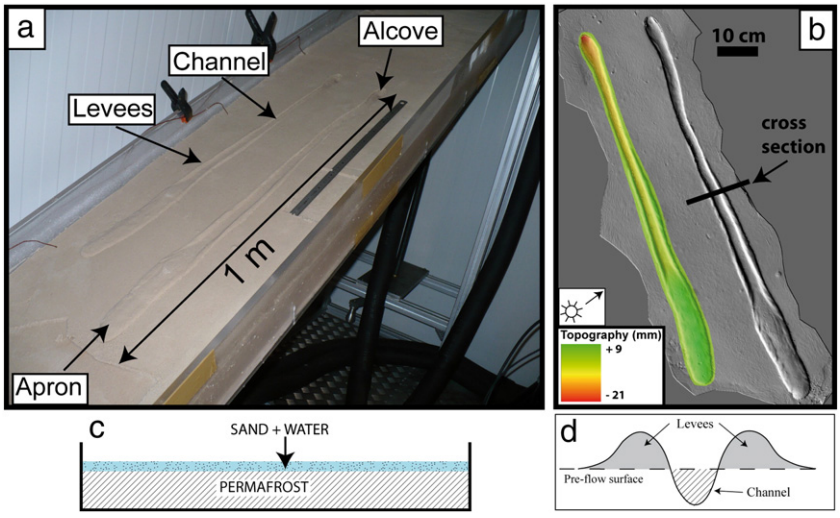

Fig. 5. Experimental results of gullies simulated in the cold room. (a) Example of two experimental flows performed in the cold room at Orsay with similar conditions (slope = 25°; volume of water used = 60 ± 10 ml; flow rate = 4.6 ml s^{-1}; thawed layer thickness = 4 mm; water content of 19% in the thawed layer). (b) Perspective hill shaded view of the DEM of the same experiment created using the laser scanner data; erosion depth and deposition thickness were calculated on the gully on the left. (c) Diagram illustrating the configuration in the cross section of the frozen bed and the wet thawed layer. (d) Schematic cross section of the deposition morphologies (levees) and erosion morphologies (channel) related to the experimental flows.

found two gullies with perched channels: they are ~10 m wide, ~1 m deep and are perched between 1 m and 2 m above the initial dune topography (Fig. 6b, d and e). On the Kaiser barchan, we have identified a perched channel on the downstream part of another gully (Fig. 6a and c). Lateral levees are well developed in the downstream part where the perched channels are observed. Upstream, the channel has eroded down into the substrate. It should be noted that the variations in the channels and gullies that are being measured here are of a scale that is near the resolution of (and therefore noise within) the topography data. Hence, it is difficult to robustly identify the perched channels, or to search for spatial patterns such as where in the channel the transition from 'normal' to 'perched' occurs. Detailed examinations of perched channels require better DEMs. Nevertheless, the profiles shown are indicative of the behavior of those gullies within the local area (about 5 m up and downstream) and we therefore conclude that there is a strong possibility that perched channels exist on Mars near the terminus of dune-gullies. In the following sections we report the results from our laboratory simulations which elucidate conditions under which such perched channels can form.

3.2. Experimental results

3.2.1. Levees, apron morphology and perched channel

The morphologies of the flows that we have generated experimentally share some key-features with Martian dune-gullies and terrestrial debris flows. A well-developed linear channel was repeatedly formed (Fig. 5) and overall width varied only slightly along the length of the flows. In every simulation, lateral levees were formed, because the center part of the flow progressed downstream faster than the lateral part of flow, leading to the deposition of sediments. Some of the eroded-sediments were also deposited at the downstream part of the flow forming a debris apron. The apron was lobate in planform, sometimes with a digitate terminus, and was linked continuously with the levees (e.g., Fig. 5a).

Of all the parameters tested, we found that only the bed-slope had a consistent effect on the apron width under both Martian and terrestrial atmospheric pressure: as the bed slope increased the apron-width decreases (Fig. 7). The decrease of the apron width for steeper slopes was observed under terrestrial and Martian atmospheric conditions (Shabesky and Matthews, 2002).

In all of our experiments the debris apron was characterized by the presence of a perched channel. In plan-view, it appears as a continuation of the 'normal' erosive channel, but its floor is above the surrounding topography. We found that a significant proportion of the deposition volume can be located below a perched channel (~5 mm thick and ~10 mm wide observed in Fig. 11).

3.2.2. Effect of atmospheric pressure

The flows produced under Mars-like atmospheric pressure were similar in terms of overall form as described in Section 3.2.1. During the creation of the experimental debris flows at low pressure, the water simultaneously boiled and froze as it flowed, as expected at these pressures and temperatures (~0 °C). Boiling occurred both on the surface of the thawed layer and also in the water flowing down the channel. When the flow was completed, this process left small-scale pits on the levees and the apron deposit (Fig. 10c, d). In some experiments, a few minutes after the flow had stopped, some of the water contained in the apron deposit and levees froze in situ although even at ~6 mbar, liquid water was observed to persist over several minutes at least 30 min in some experiments, despite being unstable at such low pressure.

Despite these effects our results showed no significant influence of the atmospheric pressure on the variation of flow morphology with slope (Section 3.2.1, Fig. 7) and in both atmospheric pressure states

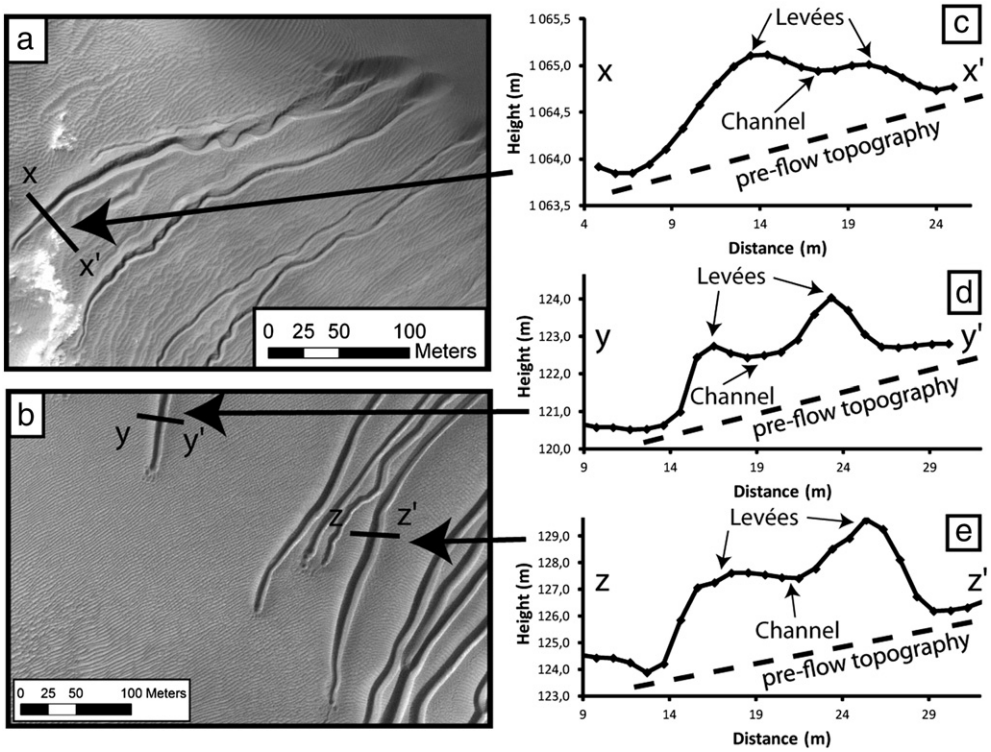

Fig. 6. Extraction of topographic cross sections in the downstream part of Martian dune gullies. (a) Image of a gully at the surface of a barchan dune located inside the Kaiser crater (HiRISE image PSP_006899_1330). (b) Image of gullies at the surface of the megadune located inside the Russell crater (HiRISE image PSP_007229_1255). (c–e) Topographic cross sections from the downstream part of the three channels, showing that the channel is elevated above the surface of the dune. The final deposits of the gully are concentrated in the levee and under the channel. The topography is extracted from the HiRISE DEM (DTEEC_006899_1330_006965_1330_U01) for the cross section c and from our HiRISE DEM (made by A. Lucas at Caltech) for the two cross sections d and e. HiRISE image credit: NASA/JPL/UofA.

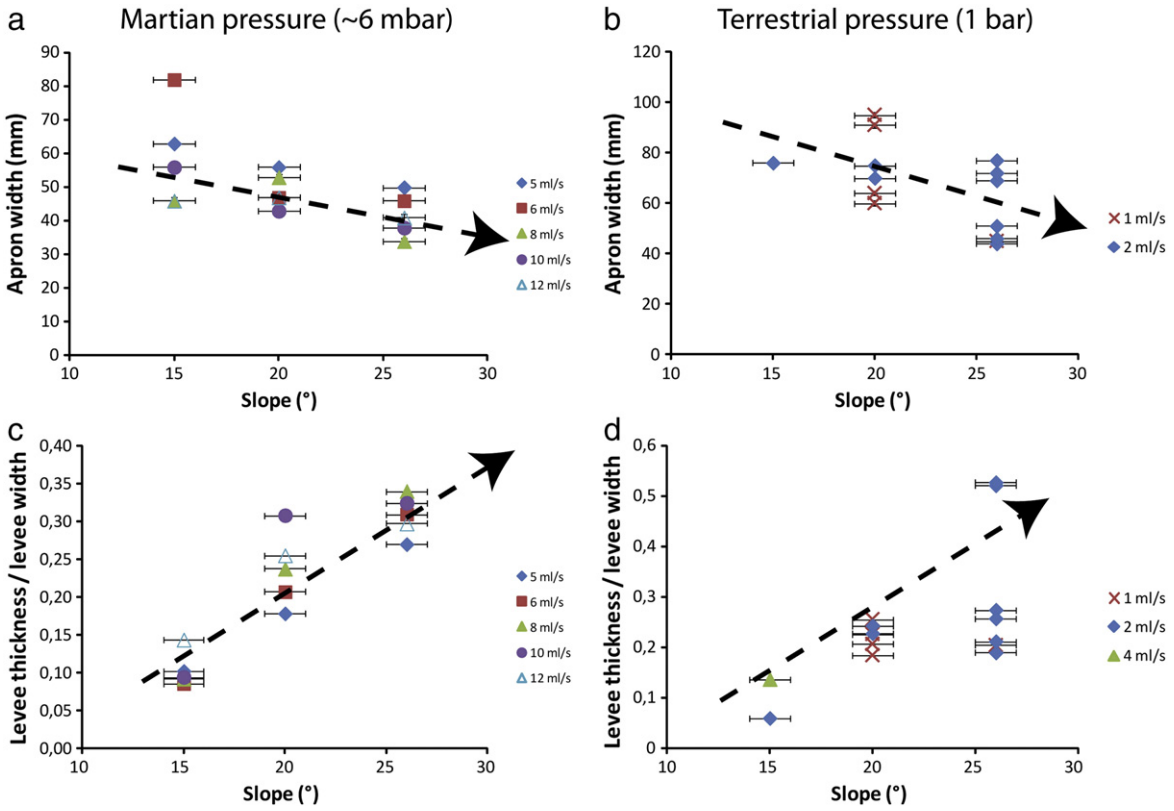

Fig. 7. Comparison between the morphology of the experimental flows performed at terrestrial atmospheric pressure and at low Martian pressure (~6 mbar). The trends are similar in both cases. (a) Apron width as a function of slope at Martian pressure. (b) Debris apron width as a function of slope at terrestrial pressure. (c–d) Ratio between levee height and levee width as a function of slope at Martian and terrestrial pressure, respectively.

perched channels were observed in the downstream part of the flow for all the experiments.

3.2.3. Effect of the thawed layer water content

We used a range of thawed layer water contents (between 0 and 23 wt.%) and a range of thawed layer thicknesses (0 to ~4 ± 1 mm; Table 1). We investigated the effect of the thawed layer's water content on the overall length of the flow (Fig. 8), the volume eroded (Fig. 9a), the volume deposited (Fig. 9b) and the length of the depositional zone, including any perched channel (Fig. 9c). In each case, increased water content in the thawed layer acts to increase the length, volume eroded, volume deposited, and the length of depositional zone of the debris flow. In these plots the length-scales and volumes have been normalized by the volume of water injected in order to account for small volume variations. A measureable increase in the overall length of the flows is observed associated with the increase of the water content of the thawed layer (Fig. 8). An increase of the water content of the thawed layer by a factor 4 resulted in an increase of the flow length by a factor of slightly more than 3.

In order to take into account the 3D dimension of the morphology and to enable comparison with features at field-scale, we included the effect of the width w and the height h of the flow (Fig. 8b). The linear dimensions ($L \gg w$) and the aspect ratio ($h \sim w$) were taken into account during the graphical analysis. The influence of the water content of the thawed layer persists when taking into account the 3D geometry of the flows. With the intention of comparing our results to Martian gullies, we have dimensioned the experimental results obtained under terrestrial conditions to account for the lower Martian gravity (Fig. 8c).

As a consequence of the positive relationship between the flow-length and the water content of the thawed layer, we observed that the volume of the eroded and deposited material were also dependent on the water content of the thawed layer. More precisely, the results showed that the increase in the volume of material eroded and deposited correlated to an increase of the water content of the thawed layer (Fig. 9a, b). This influence of the water content of the thawed layer on the volume of material eroded or deposited only seems to come into effect at higher water contents (>15% in weight).

An increase in the water content of the thawed layer also causes an increase in the length of the deposition zone (perched channel + apron) as shown in Fig. 9c. However, the length of the deposition zone increases more slowly than the overall length of the channel, so as a ratio of debris apron length to channel length, the debris apron decreases in relative size with increasing water content.

3.2.4. Eroded and deposited volumes

The deposition volume of the experimental flows ranges from ~2.2×10^5 to ~1.1×10^6 mm^3 and the erosion volume ranges from ~1.8×10^5 to ~9.8×10^5 mm^3 (Table 1). The volume of deposited material was always greater than the volume of eroded material (Fig. 10) under terrestrial atmospheric conditions, but under Martian atmospheric conditions (with volumes $<3 \times 10^5$ mm^3 for nearly half the experiments) the erosion volumes were greater than the deposition volumes.

Following re-measurement of the flow volumes after a period of desiccation (~70 h), a decrease in deposition volume was observed. Thus the discrepancy between the volume of eroded and deposited material decreased (Fig. 11). The desiccation of the wet thawed layer also modified the general appearance of the deposit area: reducing slopes and blurring the boundary between the flow and the surrounding topography (Fig. 11). This demonstrates the role water and ice contained in the deposit plays in augmenting the depositional volume.

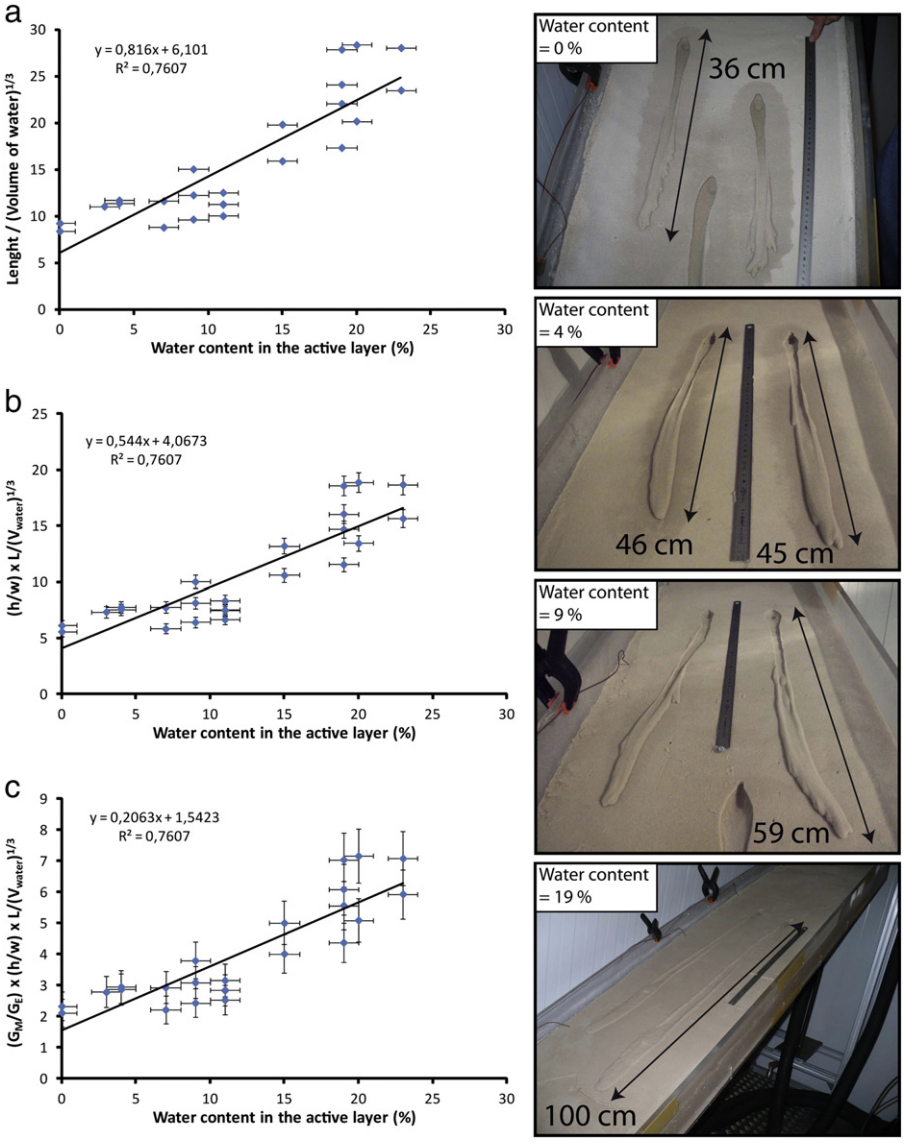

Fig. 8. Experimental results of the water content in the active layer as a function of the gully length. The water content of the thawed layer is the only parameter that changes between each experiment, the other parameters are constant (slope = 25°, flow rate = 4.6 ml·s^{-1}, thawed layer thickness = ~4 mm). The images of four different experiments on the right illustrate the trend of increasing flow-length with increasing water content inside the thawed layer. The ruler in the photographs is 50 cm in length for scale. (a) Effect of the water content in the thawed layer on the experimental flow length. The non-dimensional parameter $L/(V_{water}^{1/3})$ was used to allow comparison between experiments under Martian and terrestrial atmospheric pressure with slightly different initial water volumes. (b) Effect of the water content in the thawed layer on the flow geometry (i.e. aspect ratio between the width w, the length L and the thickness h of the debris flow). (c) Effect of the water content in the thawed layer on the flow geometry adjusted for reduced Martian gravity conditions (G_E: gravity on Earth = 9.81 m·s^{-2}; G_M: gravity on Mars = 3.71 m·s^{-2}).

4. Discussion

4.1. Mobility of flows with thawed layers

Our experiments demonstrated that the percentage of water contained in the thawed layer has an influence on the flow mobility. For example, an increase of 10% in the thawed layer water content causes an increase of 40% in the non-dimensional length of the flows (Fig. 8a). The non-dimensional length corresponds to the length of the flow (L) divided by the cube-root of the volume of water injected from the pipe ($V_{water}^{1/3}$). Hence, we account for the small variations in the volume of water injected between experiments and only the effects of the water in the thawed layer are considered. Thus it is determined that high levels of water content in the thawed layer can significantly increase the runout of a flow for any given initial volume of water.

The increased mobility of the flow with an increased proportion of water in the thawed layer can be accounted for in two ways: firstly the addition of water causes a decrease in the flow's viscosity (Coussot, 1993; Remaître et al., 2005) and hence a longer runout, and secondly it causes a decrease in infiltration capacity of the substrate, reducing loss by infiltration, which again leads to longer runout. Dealing with the first mechanism, there are two ways in which the thawed layer can contribute additional water over the length of the flow. The first is by the erosion of the thawed layer (and hence assimilation of both sand and water into the flow) along the path; the second is by gravity-driven drainage of the water from the thawed layer immediately surrounding the flow into the newly excavated void of the channel. We infer drainage of the thawed layer into the channel, because we observed water flowing into the channel after the main source had been switched off in our experiments. Hence, the water involved in the flow-formation is not necessarily sourced from the alcove area. For our experiments we have found that a significant part of the liquid (~40% of the volume, for a water content of the thawed layer of ~20%) could come from the material eroded by the flow. A basic estimation

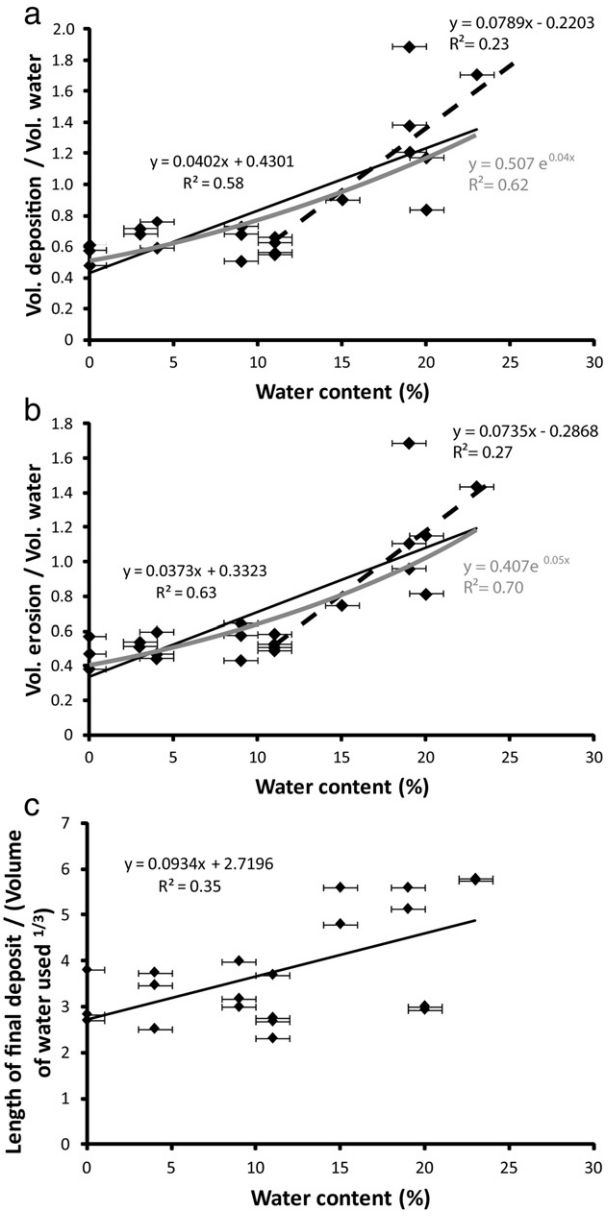

Fig. 9. Effect of the water content in the thawed layer on (a) the total volume of eroded and (b) deposited sand. The volumes of eroded and deposited material are divided by the volume of water injected from the pipe. (c) Effect of water content in the thawed layer on the length of the final deposit. The black lines and the gray lines respectively correspond to the linear fits and exponential fits including all the water content values, and the dashed lines correspond to the linear fits including only water content values ranging from 11% to 23%. The volumes of water used to generate the debris flows are between 50 and 60 ml. Slope = 25°, flow rate = 4.6 ml s^{-1}, and thawed layer thickness = ~4 mm for all the experiments.

of the concentration of liquid in the flow can be estimated using the equation

$$C_w = \left(V_{\text{fluid active layer}} + V_{\text{fluid injected}}\right) / \left(V_{\text{erosion}} + V_{\text{fluid active layer}} + V_{\text{fluid injected}}\right) \quad (1)$$

where C_w is concentration of liquid in the flow, $V_{\text{fluid active layer}}$ is the volume of liquid present inside the active layer, $V_{\text{fluid injected}}$ is the volume of liquid experimentally injected by the pipe and V_{erosion} is the volume of liquid from the material eroded by the flow.

Here we obtain a liquid concentration between 0.48 and 0.58 where the water content of the thawed layer ranges between ~20% and 23%. This liquid concentration is comparable to concentrations used in a previous experimental study concerning the runout distance of debris flows (D'Agostino et al., 2009). On Earth, a typical solid fraction of 50% to 90% has been estimated for debris flows (Corominas et al., 1996; Iverson, 1997); these values are also in line with our experiments.

The second mechanism promoting the mobility of the flow with increased water content is that of decreasing infiltration capacity. In these experiments the presence of a frozen layer already introduces a barrier to infiltration; however, if the thawed layer is not saturated, some water is lost by infiltration into this layer. If this layer is saturated, water is not lost and surface flow is favored. An increase of the length of the deposit area (perched channel + apron) with the increase of the water content into the thawed layer is observed (Fig. 9c) demonstrating that, where a perched channel is formed above the thawed layer, it is particularly difficult for water within the flow to infiltrate.

An increase in water content of the thawed layer increases the water content in the flow and engenders a decrease of the friction at the base of the flow, allowing the flow to propagate further (De Blasio, 2011). This is not simply because of the decreased viscosity of the flow. Increased pore pressures develop in the wet thawed layer as it is overridden and progressively entrained by the flow (Iverson et al., 2011). The increased pore pressure facilitates progressive scour of the bed, reduces basal friction and causes a significant flow-momentum growth (Iverson et al., 2011). The authors noted that there was a threshold response of bed-sediment pore-pressures on debris flow loading, whereby if the water content falls below a certain value then air escapes too easily to maintain pore pressures. This effect could explain the threshold at ~15% water content in Fig. 9. The water content influences on the volume deposited and eroded can be described by (1) a linear model (R^2 ~ 0.6), (2) an exponential model ($R^2 > 0.6$), (3) a linear model with a threshold at ~11% ($0.23 < R^2 < 0.27$). Further investigations are needed to determine the best model. Aquaplaning effects could also be at play and have been proposed to explain the mobility of landslides on Mars (De Blasio, 2011). The water flow above the thawed layer could permit the destabilization of the grains by a decrease of the water suction into the thawed layer and the rapid drainage of the thawed layer.

4.2. Comparability and transferability of results to Mars

The aim of this study was to understand better the apparent lack of terminal deposits of dune-gullies on Mars, but not to reproduce exactly every aspect of their dynamics and morphology. Therefore we conducted simplified experiments using homogeneous sand, smoothed topography and calibrated input whereas in reality the grain size and topography could be more heterogeneous and the input parameters highly variable.

As a consequence, the full complexity of real gullies or debris flows cannot be reproduced by our experiments. For example, heterogeneity in a flow's grain size distribution can trigger size segregation effects, which are apparent in the terminal deposits of debris flows on Earth (Johnson et al., 2012). In our experiments this effect was limited by the homogeneous grain size and by the presence of liquid water which can act to diminish the migration of large particles to the flow perimeter (Pouliquen and Vallance, 1999).

Scaling issues make it difficult to transfer terrestrial field or laboratory results to Mars (Coleman et al., 2009) or even to terrestrial debris flows (D'Agostino et al., 2009). For our experiments, we have calculated a Reynolds number ($Re = dv\rho / \mu$) between 2 and 750, by using a hydraulic radius d = 2 cm, density $1000 < \rho < 1500$ kg·m^{-3}, velocity $0.038 < v < 0.077$ m·s^{-1}, and viscosity $0.001 < \mu < 1$ Pa·s. This range of Re is in the range $250 < Re < 650$ estimated for Martian gullies using the Russell dune topographic data by Jouannic et al. (2012a). Hence, it is not unreasonable to compare morphological attributes between our experiments and the dune gullies on Mars.

In our analysis of the experimental flows' runout length (Section 4.3), we have taken into account the reduced gravity of Mars

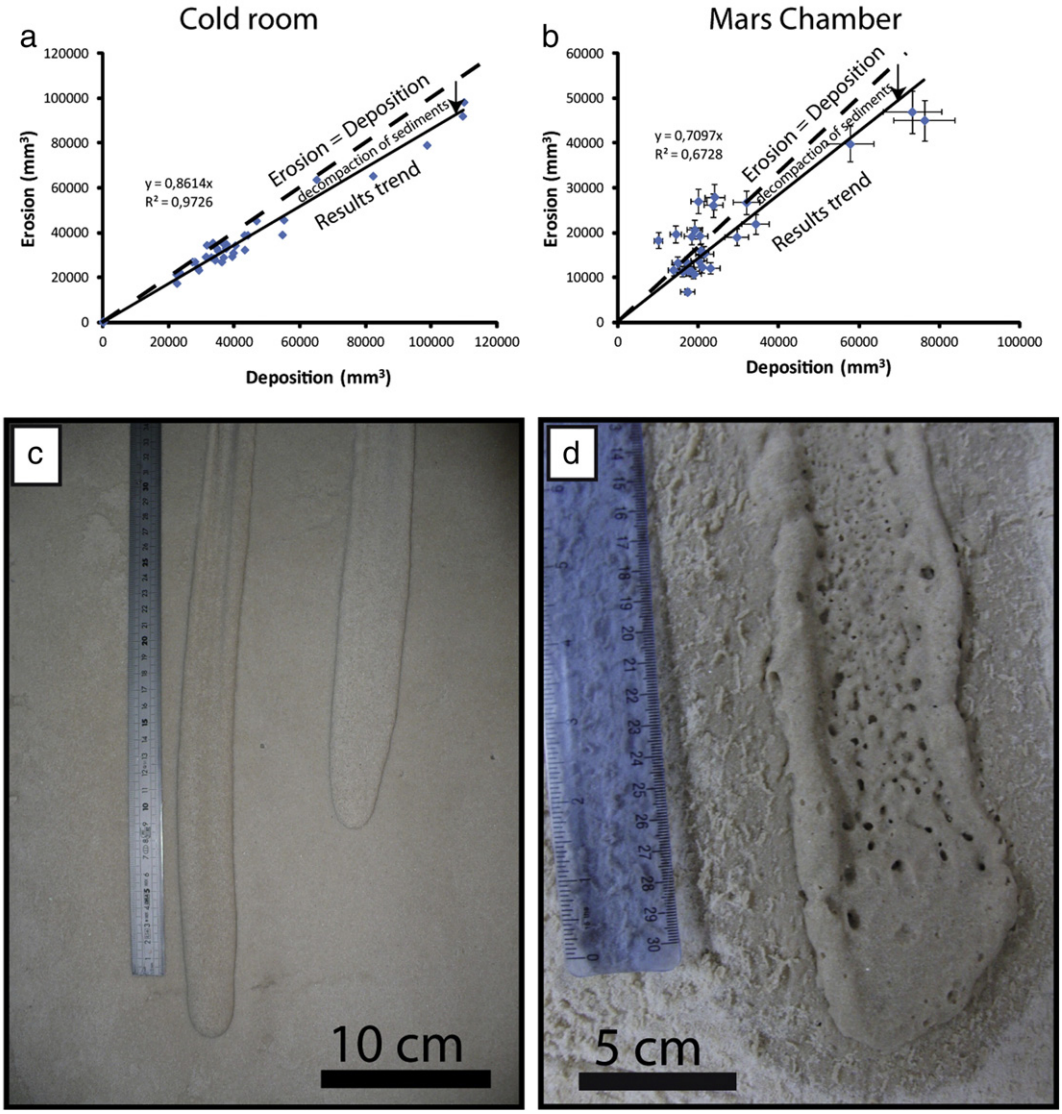

Fig. 10. Plots of the volume of erosion as a function of the volume of deposition for (a) the series of experiments in the cold room and (b) the series of experiments in the Mars Chamber (low atmospheric pressure). The dotted line represents the volume equilibrium between the erosion and the deposition and the solid line represents the calculated trend obtained from our results. The error bars concerning the volume estimations in the cold room are very small (~0.5%) and are not visible on the graph. (c) Zoomed view of the distal part of an experimental flow formed at terrestrial atmospheric pressure (1 bar); the final deposits are compact and the surface is smooth. (d) Zoomed view of the distal part of an experimental flow formed at Martian atmospheric pressure (~6 mbar), showing the presence of small pits in the final deposits.

using non-dimensional parameters (Fig. 8c), but secondary effects due to possible modification of the dynamic friction angle (Kleinhans et al., 2011; Sullivan et al., 2011) have been neglected. Only the atmospheric pressure has been tested. The influence of the atmosphere composition on the morphology was not tested. This probably influenced the rate of evaporation, freezing and sublimation.

We have focused our study on wet flow over a frozen substrate. Nevertheless, dry granular flows can also generate several surface features (levees, channels) superficially similar to those seen in Martian gullies (Shinbrot et al., 2004). During our experiments, no significant sinuosity was observed, whereas this is observed in dune gullies on Mars (e.g., Mangold et al., 2003) and in debris flows on Earth. On Earth, topographic heterogeneity is likely to be responsible for sinuosity in debris flow paths, as illustrated by a sinuous debris flow in the Vallée de la Clarée (Fig. 2c, French Alps) caused by the presence of trees along its path. Hence, the lack of sinuosity in our experimental flows can be attributed to the simplified topography, rather than a dissimilarity of process.

4.3. Application to Martian dune gullies

HiRISE elevation data have been used to measure the morphology and estimate the initial water volume necessary to generate gullies on the Russell megadune. These gullies are 2 km long, located on a gentle slope (10–15°), with a depth of approximately ~1 m, channel width of ~10 m, levee height range between 0.5 and 1.8 m and levee width range between ~3–15 m (Mangold et al., 2003; Reiss and Jaumann, 2003; Jouannic et al., 2012a). The water volume necessary to produce such phenomena has been estimated to be 4500–7000 m^3 by Jouannic et al. (2012a), but the same authors found that the volume of the reservoir located at the top of the sand dune was only of 400–900 m^3. This provides a conundrum. However, by using the experimental results presented here, we can provide some explanations for this mismatch. If we scale our non-dimensional experimental results for flow length (using the linear interpolation obtained in Fig. 8c; Martian gravity = 3.7 m s^{-2}; Earth gravity = 9.8 m s^{-2}) and use a reservoir volume of ~900 m^3, we can obtain a gully with a length of 2 km as observed on

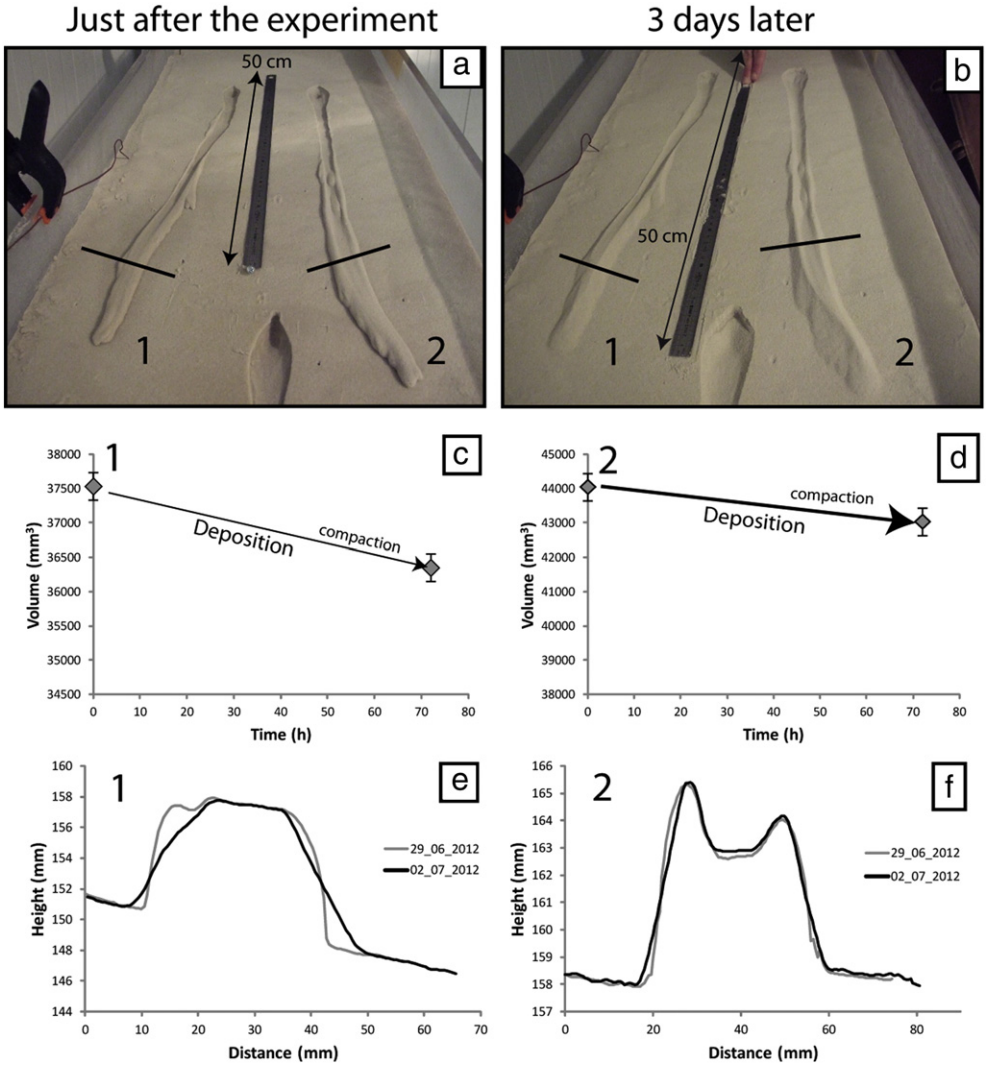

Fig. 11. Effect of desiccation of the superficial layer on the morphology of experimental flows. (a) Image of the morphology just after the experiment. (b) Image of the morphology three days after the experiment. (c and d) Evolution of total deposition volume for the flows labeled 1 and 2 in a and b as a function of time. (e and f) Evolution of the topographic cross-section from 29 June 2012 (gray curve) to 2 July 2012 (black curve) for the flows labeled 1 and 2 in a and b. The ruler on the pictures is 50 cm in length for scale. Slope = 25°, flow rate = 4.6 ml·s^{-1}, and initial thawed layer thickness = ~4 mm.

Russell megadune on Mars. In this calculation we assume the flow propagates in a channel ~10 m wide, above a sandy substrate containing 30% of liquid water in an upper thawed layer of ~1 m in thickness, with a slope of 10°. In other words, over the relatively shallow slope of dunes on Mars, with a relatively small initial volume of liquid, a flow could propagate over much longer distances than expected for dry sand, if it occurs on a substrate composed of wet sediments overlying a frozen base. However, the conditions that produced such an active layer (obliquity or seasonal activity) are beyond the scope of this paper.

4.4. Deposit morphology and degradation of morphology

On Earth and Mars, many gully morphologies result from the succession of multiple flow events and the progressive accumulation of sediments in the downstream part of gullies (Fig. 1a, d). In these cases, a large terminal debris apron deposit can be observed (Hugenholtz et al., 2007) and such an apron can be obtained experimentally by superposition of successive flow events. There is also a less abundant category of debris flow morphologies that is characterized by reduced terminal deposit or the apparent lack of deposit. On Earth, these small terminal deposits of debris flows can be found in cold and periglacial environment on scree slopes (French Alps; Jomelli et al., 2007) or on slopes of volcanoes with very fine sediments (Fig. 1b; Italy). On Mars, small terminal deposits have been found in gullies on the inner wall of Tooting crater (Fig. 1e) and in dune gullies (e.g. the Matara and Russell crater dunes studied here), which we show also have a perched channel in the downstream part of the gullies. Our results show that small terminal deposits can be simulated experimentally under periglacial conditions using an ice-rich substrate composed of fine sand (200–250 μm) beneath a thin thawed layer containing a high proportion of water (~10–20% in weight) under low (6 mbar) or ambient (1 bar) pressure conditions (Fig. 10). A large proportion of the terminal deposits are located in the area where perched channels develop, hence can easily be confused for erosional morphology in plan view. The aspect ratio between the width w and the length L of deposits (perched channel + apron) for our experiments ranges between $1/22 < W/L < 1/10$, which is very similar to that of gullies on the Russell crater megadune (~1/20; Jouannic et al., 2012a) or on Kaiser crater dunes (~1/6; Gargani et al., 2012).

Our experiments show that the degradation of the flow morphology, due to the desiccation of the surface over time, decreases the measured volume of the deposits and degrades their appearance (Fig. 11). The fresh morphology of the experimental flows is characterized by complex lobate features with steep local slopes on the inner and outer

parts of the levees: such features are not observed on Martian dune gullies. After desiccation, we observed that the deposits lose their cohesion, becoming smoother and less complex (Fig. 11b). This is a direct result of the angle of repose (i.e. angle of friction) for dry sand being smaller than the angle of repose for wet sand (Rist et al., 2012). Hence, the sand grains are displaced by their own weight and compaction occurs reversing some of the decompaction that took place with erosion (Fig. 10). This initial decompaction is a result of non-optimal reorganization of the sand grains (presence of bubbles and space between grains; Fig. 10d), which then settle on desiccation. Despite the loss of fine-scale morphology of our experimental flows during desiccation, they retained the topographic signature of levees and perched channels (Fig. 11c, d). The change in morphology of our experimental flows on desiccation renders them more similar to the dune gullies observed on Mars. Hence, a lack of some of the fine-scale morphologies exhibited by our experimental flows in the Martian examples could be simply due to desiccation processes. In addition the loss of definition of the outer-edge of the levees could explain why perched channels had not been previously identified on Martian dune gullies.

5. Conclusions

In spite of the numerous processes that could explain the formation of gullies and their dynamics (e.g. runoff, debris flows, granular flows, and sliding CO_2 blocks), we focus in this work on the role of liquid contained in the substrate as well as on the liquid flow and choose to experimentally test the plausibility of this hypothesis. The results of this work do not rule out the possibility that other processes could have formed linear gullies on Martian dunes. In conclusion, this work demonstrated that:

- The presence of a thin thawed or water-rich layer above a sedimentary substrate containing ground ice could explain why dune gullies on Mars and other debris flows on Earth have small terminal deposits, long runout distances (for relatively low slopes) and the presence of a 'perched' channel.
- We suggest that water from the thawed layer is incorporated progressively into the flow during progression, which reduces its viscosity. Furthermore, the presence of high water content in the thawed layer reduces infiltration of the flow into it, and possibly reduces friction at the base of the flow. These act to increase the runout length for a given initial volume of water. This additional source of water could explain the extremely long runout of dune gullies on Mars, compensating for their small upslope reservoir.
- Although absolute apron length increases with water content in the thawed layer, this effect is less than the increase in the length of the entire flow. Hence, fractional debris apron length decreases with the water content of the substrate. This could provide another explanation for the abbreviated terminal deposits observed in Martian dune gullies.
- Atmospheric pressure seems to have little influence on the length, apron-width and levee aspect ratio of the simulated debris flows.
- Our study highlights the potential role of post-emplacement degradation on the morphology of debris flows in sand. Post-formation desiccation can decrease the volume of the flow, and 'blur' the outer margins of the levees, making them hard to identify in remote sensing images.
- The apparent small size of the terminal deposits associated with Martian dune gullies is also a function of observational bias: the presence of a perched channel, which is a depositional feature, cannot be detected in plan-view images. If many dune gullies possess perched channels, this has a bearing on potential formation hypotheses, as 'dry' formational hypotheses are based on the assumption that such gullies have truncated terminal deposits.
- Future studies should aim to use the highest quality DEM data to search for more evidence for perched channels, and to explore how the balance between erosion and deposition of sediment evolves along flow. This will help constrain formation mechanisms for dune gullies on Mars.

Acknowledgment

This work is supported by "Programme National de Planétologie" from the CNRS-INSU and the CNES—MarsExpress program and the HRSC team that provided the data. G.J., J.G. and S.J.C. received a Europlanet transnational access grant for the experiment in the OU Mars Chamber. We thank Laureen Fenech for her technical support in the cold room (Orsay, Univ. Paris Sud) for four months in 2011. We thank A. Lucas for the compilation of the Russell dune DTM. LiDAR and aerial photography data for the Ísafjörður site in northwestern Iceland were obtained from the UK Natural Environment Research Council Airborne Research and Survey Facility (NERC ARSF) project IG13/11, PI: Susan Conway. We thank the two anonymous reviewers and Takashi Oguchi for their useful comments, thorough and helpful reviews.

References

Aston, A.H., Conway, S.J., Balme, M.R., 2011. Identifying Martian gully evolution. In: Balme, M., Bargery, A.S., Gallagher, C., Gupta, S. (Eds.), Martian Geomorphology. The Geological Society of London 356, pp. 151–169.

Balme, M., Mangold, N., Baratoux, D., Costard, F., Gosselin, M., Masson, P., Pinet, P., Neukum, G., 2006. Orientation and distribution of recent gullies in the southern hemisphere of Mars: Observations from High Resolution Stereo Camera/Mars Express (HRSC/MEX) and Mars Orbiter Camera/Mars Global Surveyor (MOC/MGS) data. J. Geophys. Res. 111 (E05001).

Cedillo-Flores, Y., Treiman, A.H., Lasue, J., Clifford, S.M., 2011. CO_2 fluidization in the initiation and formation of Martian polar gullies. Geophys. Res. Lett. 38, L21202. http://dx.doi.org/10.1029/2011GL049403.

Chevrier, V.F., Ulrich, R., Altheide, T.S., 2009. Viscosity of liquid ferric sulfate solutions and application to the formation of gullies on Mars. J. Geophys. Res. 114, E06001. http://dx.doi.org/10.1029/2009JE003376.

Christensen, P.R., 2003. Formation of recent Martian gullies through melting of extensive water-rich snow deposits. Nature 422, 45–48.

Coe, J.A., Godt, J.W., Henceroth, A.J., 2002. Debris Flows Along the Interstate 70 Corridor, Floyd Hill to the Arapahoe Basin Ski Area, Central Colorado — A Field Trip Guidebook U.S. Geological Survey Open-File Report 02-398.

Coleman, K.A., Dixon, J.C., Howe, K.L., Roe, L.A., Chevrier, V., 2009. Experimental simulation of Martian gully forms. Planet. Space Sci. 57, 711–716.

Conway, S.J., Decaulne, A., Balme, M.R., Murray, J.B., Towner, M.C., 2010. A new approach to estimating hazard posed by debris flows in the Westfjords of Iceland. Geomorphology 114, 556–572.

Conway, S.J., Balme, M.R., Murray, J.B., Towner, M.C., Okubo, C.H., Grindrod, P.M., 2011a. The indication of Martian gully formation processes by slope–area analysis. In: Balme, M., Bargery, A., Gallagher, C., Gupta, S. (Eds.), Martian Geomorphology. Geological Society of London, Special Publications 356, pp. 171–201.

Conway, S.J., Lamb, M.P., Balme, M.R., Towner, M.C., Murray, J.B., 2011b. Enhanced runout and erosion by overland flow at low pressure and sub-freezing conditions: experiments and application to Mars. Icarus 211, 443–457.

Corominas, J., Remondo, J., Farias, P., Estevao, M., Zezere, J., Dias de Teran, J., Dikau, R., Schrott, L., Moya, J., Gonzalez, A., 1996. Debris flow. In: Dikau, R., et al. (Eds.), Landslide Recognition. John Wiley, New York, pp. 161–180.

Costard, F., Forget, F., Mangold, N., Peulvast, J.P., 2002. Formation of recent Martian debris flows by melting of near-surface ground ice at high obliquity. Science 295, 110–113.

Coussot, P., 1993. Rhéologie des boues et laves torrentielles – Étude de dispersions et suspensions concentrées. Centre d'Étude du Machinisme Agricole des Eaux et Forêts, Laboratoire de rhéologie, Grenoble, p. 415.

Coussot, P., Meunier, M., 1996. Recognition, classification and mechanical description of debris flows. Earth Sci. Rev. 40, 209–227.

D'Agostino, V., Cesca, M., Marchi, L., 2009. Field investigations of runout distances of debris flows in the Dolomits (Eastern Italian Alps). Geomorphology 116, 294–304.

De Blasio, V., 2011. The aureole of Olympus Mons (Mars) as the compound deposit of submarine landslides. Earth Planet. Sci. Lett. 312, 126–139.

Dickson, J.L., Head, J.W., Kreslavsky, M., 2007. Martian gullies in the southern midlatitudes of Mars: evidence for climate-controlled formation of young fluvial features based upon local and global topography. Icarus 188, 315–323.

Diniega, S., Hansen, C.J., McElwaine, J.N., Hugenholtz, C.H., Dundas, C.M., McEwen, A.S., Bourke, M.C., 2013. A new dry hypothesis for the formation of Martian linear gullies. Icarus 225, 526–537.

Ferrucci, M., Pertusati, S., Sulpizio, R., Zanchetta, G., Pareschi, M.T., Santacroce, R., 2005. Volcaniclastic debris flows at La Fossa Volcano (Vulcano Island, southern Italy): insights for erosion behaviour of loose pyroclastic material on steep slopes. J. Volcanol. Geotherm. Res. 145, 173–191.

Gaidos, E.J., 2001. Cryovolcanism and the recent flow of liquid water on Mars. Icarus 153, 218–223.

Gargani, J., Jouannic, G., Costard, F., Ori, G., Marmo, C., Schmidt, F., Lucas, A., Busson, J., 2012. How much liquid water was there on Martian dunes? EGU abstract, Vienna, p. 11720.
Hartmann, W.K., 2001. Martian seeps and their relation to youthful geothermal activity. Space Sci. Rev. 96, 405–410.
Hauber, E., Reiss, D., Ulrich, M., Preusker, F., Trauthan, F., Zanetti, M., Hiesinger, H., Jaumann, R., Johansson, L., Johnsson, A., Van Gasselt, S., Olvmo, M., 2011. Landscape evolution in Martian mid-latitude regions: insights from analogous periglacial landforms in Svalbard. In: Balme, M., Bargery, A., Gallagher, C., Gupta, S. (Eds.), Martian Geomorphology, Geological Society of London, Special Publications 356, pp. 111–131.
Heldmann, J.L., Mellon, M.T., 2004. Observations of Martian gullies and constraints on potential formation mechanisms. Icarus 168, 285–304.
Hoffman, N., 2002. Active polar gullies on Mars and the role of carbon dioxide. Astrobiology 2, 313–323.
Hooper, D.M., Dinwiddie, C.L., 2014. Debris flows on the Great Kobuk Sand Dunes, Alaska: implications for analogous processes on Mars. Icarus 230, 15–28.
Horgan, B.H.N., Bell III, J.F., 2012. Seasonally active slipface avalanches in the north sand sea of Mars: evidence for a wind-related origin. Geophys. Res. Lett. 39, L09201. http://dx.doi.org/10.1029/2012GL051329.
Hugenholtz, C.H., Wolfe, S.A., Moorman, B.J., 2007. Sand–water flows on cold-climate eolian dunes: environmental analogs for the eolian rock record and Martian sand dunes. J. Sediment. Res. 77, 607–614.
Ishii, T., Sasaki, S., 2004. Formation of recent Martian gullies by avalanches of CO_2 frost. Lunar Planet. Sci. 35 (Abstract 1556).
Iverson, R.M., 1997. The physics of debris flows. Rev. Geophys. 35, 245–296.
Iverson, R.M., Reid, M.E., Logan, M., LaHusen, R.G., Godf, J.W., Griswold, J.P., 2011. Positive feedback and momentum growth during debris-flow entrainment of wet bed sediment. Nat. Geosci. 4, 116–121. http://dx.doi.org/10.1038/NGEO1040.
Johnson, C.G., Kokelaar, B.P., Iverson, R.M., Logan, M., LaHusen, R.G., Gray, J.M.N.T., 2012. Grain-size segregation and levee formation in geophysical mass flows. J. Geophys. Res. 117, F01032. http://dx.doi.org/10.1029/2011JF002185.
Jomelli, V., Francou, B., 2000. Comparing the characteristics of rockfall talus and snow avalanche landforms in an Alpine environment using a new methodological approach: Massif des Ecrins, French Alps. Geomorphology 35, 181–192.
Jomelli, V., Brunstein, D., Grancher, D., Pech, P., 2007. Is the response of hill slope debris flows to recent climate change univocal? A case study in the Massif des Ecrins (French Alps). Climate Change 85, 119–137.
Jouannic, G., Gargani, J., Costard, F., Ori, G.G., Marmo, C., Schmidt, F., Lucas, A., 2012a. Morphological and mechanical characterization of gullies in a periglacial environment: the case of the Russell dune (Mars). Planet. Space Sci. 71, 38–54.
Jouannic, G., Conway, S.J., Gargani, J., Costard, F., Patel, M.R., Ori, G.G., 2012b. Experimental investigation of gully formation under low pressure and low temperature conditions. Lunar Planet. Sci. 43 (Abstract 1509).
Kirk, R.L., Howington-Kraus, E., Rosiek, M.R., Anderson, J.A., Archinal, B.A., Becker, K.J., Cook, D.A., Galuszka, D.M., Geissler, P.E., Hare, T.M., Holmberg, I.M., Keszthelyi, L.P., Redding, B.L., Delamere, W.A., Gallagher, D., Chapel, J.D., Eliason, E.M., King, R., McEwen, A.S., 2008. Ultrahigh resolution topographic mapping of Mars with MRO HiRISE stereo images: meter-scale slopes of candidate Phoenix landing sites. J. Geophys. Res. 113, E00A24. http://dx.doi.org/10.1029/2007JE003000.
Kleinhans, M.G., Markies, H., de Vet, S.J., in't Veld, A.C., Posterma, F.N., 2011. Static and dynamic angles of repose in loose granular materials under reduced gravity. J. Geophys. Res. 116, E11004. http://dx.doi.org/10.1029/2011JE003865.
Knauth, L.P., Burt, D., 2003. Electrically conducting Ca-rich brines, rather than water, expected in the Martian subsurface. Geol. Soc. Am. Bull. 115, 566–580.
Knauth, L.P., Klonowski, S., Burt, D., 2000. Ideas about the surface runoff features on Mars. Science 290, 711–712.
Kolb, K.J., McEwen, A.S., Pelletier, J.D., 2010. Investigating gully flow emplacement mechanisms using apex slopes. Icarus 208, 132–142.
Lanza, N.L., Meyer, G.A., Okubo, C.H., Newsom, H.E., Wiens, R.C., 2010. Evidence for debris flow gully formation initiated by shallow subsurface water on Mars. Icarus 205, 103–112.
Larsson, S., 1982. Geomorphological effects on the slopes of Longyear Valley, Spitsbergen, after a heavy rainstorm in July 1972. Geogr. Ann. Ser. A Phys. Geogr. 64, 105–125.
Malin, M.C., Edgett, K.S., 2000. Evidence for recent groundwater seepage and surface runoff on Mars. Science 288, 2330–2335.
Mangold, N., Costard, F., Forget, F., 2003. Debris flows over sand dunes on Mars: evidence for liquid water. J. Geophys. Res. 108, 5027. http://dx.doi.org/10.1029/2002JE001958.
Mangold, N., Mangeney, A., Migeon, V., Ansan, V., Lucas, A., Baratoux, D., Bouchut, F., 2010. Sinuous gullies on Mars: frequency, distribution, and implications for flow properties. J. Geophys. Res. 115, E11001. http://dx.doi.org/10.1029/2009JE003540.
Mattson, S., McEwen, A.S., Ojha, L., Heyd, R., Howington-Kraus, E., Kirk, R.L., 2011. High resolution digital models and orthorectified images of Mars from HiRISE and HiSCI. EuroPlanet 5 (Abstract 1380).
McDonald, R., Andersen, R.S., 1996. Constraints on eolian grain flow dynamics through laboratory experiments on sand slopes. J. Sediment. Res. 66, 642–653.
McEwen, A.S., Hansen, C.J., Delamere, W.A., Eliason, E.M., Herkenhoff, K.E., Keszthetyi, L., Gulick, V.C., Kirk, R.L., Mellon, M.T., Grant, J.A., Thomas, N., Weitz, C.M., Squyres, S.W., Bridges, N.T., Murchie, S.L., Seelos, F., Seelos, K., Okubo, C.H., Milazzo, M.P., Tornabene, L.L., Jaeger, W.L., Byrne, S., Russell, P.S., Griffes, J.L., Martínez-Alonso, S., Davatzes, A., Chuang, F.C., Thomson, B.J., Fishbaugh, K.E., Dundas, C.M., Kolb, K.J., Banks, M.E., Wray, J.J., 2007. Mars Reconnaissance Orbiter's High Resolution Imaging Science Experiment (HiRISE). J. Geophys. Res. 112, E05S02. http://dx.doi.org/10.1029/2005JE002605.
Morris, A.R., Mouginis-Mark, P.J., Garbeil, H., 2010. Possible impact melt and debris flows at Tooting Crater, Mars. Icarus 209, 369–389.
Musselwhite, D.S., Swindle, T.D., Lunine, J.I., 2001. Liquid CO_2 breakout and the formation of recent small gullies on Mars. Geophys. Res. Lett. 28, 1283–1285.
Pelletier, J.D., Kolb, K.J., McEwen, A.S., Kirk, R.L., 2008. Recent bright gully deposits on Mars: wet or dry flow? Geology 36, 211–214.
Pouliquen, O., Vallance, J.W., 1999. Segregation induced instabilities of granular fronts. Chaos 9, 621–630.
Reiss, D., Jaumann, R., 2003. Recent debris flows on Mars: seasonal observations of the Russell Crater dune field. Geophys. Res. Lett. 30. http://dx.doi.org/10.1029/2002GL016704.
Remaître, A., Malet, J.P., Maquaire, O., Ancey, C., Locat, J., 2005. Flow behaviour and runout modelling of a complex debris flow in clay-shales basin. Earth Surf. Process. Landf. 30, 479–488.
Rist, A., Philips, M., Springman, S.M., 2012. Inclinable shear box simulations of deepening active layers on perennially frozen scree slopes. Permafr. Periglac. Process. 23, 26–38.
Sattler, K., Keiler, M., Zischg, A., Schron, L., 2011. On the connection between debris flow activity and permafrost degradation: a case study from Schnalstal, South Tyrolean Alps, Italy. Permafr. Periglac. Process. 22, 254–265.
Shabesky, R.A., Matthews, J.A., 2002. Sieve deposition by debris flow on a permeable substrate, Leirdalen, Norway. Earth Surf. Process. Landf. 27, 1031–1041.
Shinbrot, T., Duong, N.H., Kwan, L., Alvarez, M.M., 2004. Dry granular flows can generate surface features resembling those seen in Martian gullies. PNAS 101, 8542–8546.
Sullivan, R., Anderson, R., Biesiadecki, J., Bond, T., Stewart, H., 2011. Cohesions, friction angles, and other physical properties of Martian regolith from Mars Exploration Rover wheel trenches and wheel scuffs. J. Geophys. Res. 116, E02006. http://dx.doi.org/10.1029/2010JE003625.
Sutton, S.L.F., McKenna, N., Neuman, C., Nickling, W., 2013a. Lee slope sediment processes leading to avalanche initiation on an Aeolian dune. J. Geophys. Res. 118, 1754–1766.
Sutton, S.L.F., McKenna Neuman, C., Nickling, W., 2013b. Avalanche grainflow on a simulated Aeolian dune. J. Geophys. Res. 118, 1767–1776.
Védie, E., Costard, F., Font, M., Lagarde, J.L., 2008. Laboratory simulations of Martian gullies on sand dunes. Geophys. Res. Lett. 35, L21501. http://dx.doi.org/10.1029/2008GL035638.
Williams, K.E., Toon, O.B., Heldmann, J.L., Mellon, M.T., 2009. Ancient melting of mid-latitude snowpacks on Mars as a water source for gullies. Icarus 200, 418–425.
Winkelbach, S., Molkenstruck, S., Wahl, F., 2006. Low-cost laser range scanner and fast surface registration approach. In: Franke, K., Müller, K.-R., Nickolay, B., Schäfer, R. (Eds.), Pattern Recognition, Lecture Notes in Computer Science. Springer, Berlin Heidelberg, pp. 718–728.